

Structure and properties of liquid InSb alloy below and above the melting point: *ab initio* molecular dynamics simulations

This article has been downloaded from IOPscience. Please scroll down to see the full text article.

2006 J. Phys.: Condens. Matter 18 4471

(<http://iopscience.iop.org/0953-8984/18/19/003>)

View [the table of contents for this issue](#), or go to the [journal homepage](#) for more

Download details:

IP Address: 129.252.86.83

The article was downloaded on 28/05/2010 at 10:39

Please note that [terms and conditions apply](#).

Structure and properties of liquid InSb alloy below and above the melting point: *ab initio* molecular dynamics simulations

Y N Wu, G Zhao, C S Liu¹ and Z G Zhu

Key Laboratory of Material Physics, Institute of Solid State Physics, Chinese Academy of Sciences, PO Box 1129, Hefei 230031, People's Republic of China

E-mail: cslu@issp.ac.cn

Received 10 January 2006

Published 25 April 2006

Online at stacks.iop.org/JPhysCM/18/4471

Abstract

Using *ab initio* molecular dynamics simulations, we have investigated the structure, diffusion and electronic properties of liquid InSb alloy below and above the melting point. A large gap in value or a 'flat shape' between the position of the first and second peak of the calculated pair correlation function, and an asymmetry of the first peak, were displayed in our simulations. There is a small hump between the first and second peak of the partial pair correlation function of Sb atoms, which gradually disappears with increasing temperature. Analysis of the compositional disorder number suggests that heterogeneous bonds still play a predominant role in liquid InSb alloy. With increasing temperature, the opened chain-like Sb–Sb bonds are broken and the Peierls distortion of Sb atoms in liquid InSb alloy is weakened. With the change of temperature, the diffusion coefficients obtained from the average mean-square displacement can be fitted by the Arrhenius equation. The fit yields an activation energy of 0.20 eV and a pre-exponential factor of $2.01 \times 10^{-8} \text{ m}^2 \text{ s}^{-1}$.

1. Introduction

Temperature-induced changes in the structure and physical properties of materials are of fundamental interest in condensed matter physics. Because of experimental difficulties and limited structural information, liquid matter has not been investigated as much as crystalline matter. Recently, liquid InSb alloy has attracted a great deal of attention due to its evolution of chemical bonding and abnormal physical properties [1–4]. InSb is one of the popular III–V covalent semiconductors. In crystalline InSb (c-InSb), the In–Sb bond has a weak ionic character, and its Phillips ionicity is 0.32 [5]. At ambient conditions, c-InSb has a zinc blende structure with a coordinate number of 4 at a distance 0.2835 nm. Molecular dynamics study

¹ Author to whom any correspondence should be addressed.

shows amorphous InSb to have a structure of two- and threefold rings [6]. The melting point of InSb is 783 K [7]. Upon melting, because the thermal motion of atoms breaks some of the covalent bonds, compositional defects or ‘wrong’ bonds exist (bonds between the same type of atom are absent in the crystalline state). The local structure of liquid InSb (l-InSb) shows a correlation between the short and long bonds for Sb atoms as in l-Sb [1], which shows a weak Peierls distortion [8].

One of the most important properties of a liquid is its viscosity. Glazov *et al* [9] reported results for the viscosity of l-InSb in pioneering work done in the late 1960s on liquid semiconductors. They measured the dependence of the viscosity with temperature following non-Arrhenius behaviour. However, Sato *et al* [10] used an oscillating viscometer to measure the viscosity of l-InSb using a specially designed quartz crucible to prevent the evaporation of Sb from the melts, and found that the viscosity of l-InSb showed good Arrhenius linearity from a supercooled temperature to about 1340 K.

Ab initio molecular dynamics (AIMD) simulations have been proved to be very reliable for the prediction of structural changes and electronic properties of l-Sb, l-InSb and amorphous InSb [1, 2, 6, 8]. In this paper we will perform AIMD simulations based on density-functional theory (DFT) and the pseudopotential method to study the properties of l-InSb below and above the melting point. First, we will investigate structural changes of l-InSb from a supercooled temperature of 700 to 1339 K. Second, we will study the dependence of the diffusion coefficient on temperature for l-InSb. Finally, we will study the electronic structure of supercooled liquid and normal liquid InSb in the hope of gaining an understanding of the metallic-like behaviour from undercooled liquid to normal liquid.

2. Computational methods

We have carried out first-principles simulations of l-InSb using the *ab initio* total energy and molecular dynamics program VASP [11, 12], in which the interactions between the ions and electrons are described by ultrasoft pseudopotentials (USPP) of the Vanderbilt type. We dealt with the electronic exchange and correlation using the generalized gradient approximation (GGA). Our GGA calculations use the PW91 functional due to Perdew and Wang [13]. Minimization of the total energy was performed using an efficient matrix diagonalization scheme based on the conjugate-gradient technique [14].

We considered a system with 80 atoms in a cubic box with periodic boundary conditions. Only Γ -point sampling was used to sample the supercell Brillouin zone. We first built a system of density 6.18 g cm^{-3} at an experimental temperature of 1339 K [9]. All the dynamical simulations were performed in a canonical ensemble with a *Nosé* thermostat [15] to control the temperature. Newton’s equations of motion were integrated using the Verlet algorithm [16] with a time step of 3 fs. In order to eliminate any ‘memory’ effect from the initial configuration, the system was thermalized at a temperature of 3000 K for 3 ps. After randomization at the elevated temperature, we gradually cooled the system to a temperature of 1339 K for 3 ps. After equilibration, we acquired structural information during another 12 ps in which the energy conservation was excellent. This procedure was repeated for subsequent temperatures. The size of box was adjusted in order to maintain the variation of external pressure at the different temperatures within 5 kbar, corresponding to a 0.1% or smaller volume change.

3. Results and discussions

3.1. Structural properties

The pair correlation function, $g(r)$, is an important physical quantity in the physics of fluids because it is directly measurable and, in principle, various properties of liquid materials can be

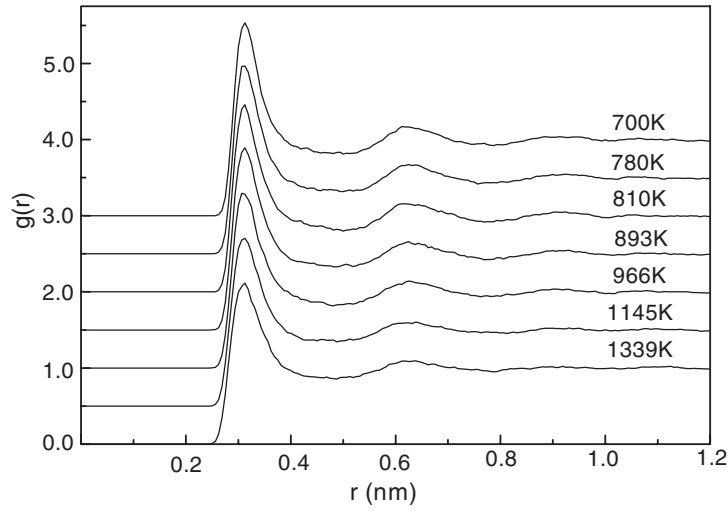


Figure 1. The pair correlation functions of liquid InSb alloy.

estimated from the pair correlation function when coupled with an appropriate theory. Using the atomic coordinates from the molecular dynamics simulations, the total pair correlation functions of l-InSb, shown in figure 1, were calculated at seven different temperatures ranging from 700 to 1339 K. As can be seen from figure 1, a large gap in value or a ‘flat shape’ between the positions of the first and second peak, and an asymmetry of the first peak, were displayed in our simulations. The first peak position (r_1) is around 0.313 nm, which is not sensitive to temperature. The second peak position (r_2) shifts toward a larger r value as temperature is raised. Consequently, the ratio of r_2/r_1 becomes smaller with decreasing temperature. Although the height of the first and second peaks increases as temperature decreases, the ratio of $g(r_2)/g(r_1)$ decreases. The first peak gradually becomes broader with increasing temperature.

The partial pair correlation functions $g_{\text{InIn}}(r)$, $g_{\text{InSb}}(r)$ and $g_{\text{SbSb}}(r)$ were also calculated and are shown in figure 2. The first peak positions of $g_{\text{InIn}}(r)$, $g_{\text{InSb}}(r)$ and $g_{\text{SbSb}}(r)$ are around 0.313, 0.309 and 0.302 nm, respectively, which are almost invariable with the variation of temperature. The heights of the first and the second peaks decrease with increasing temperature. For $g_{\text{SbSb}}(r)$, there exists a small hump between the first and second peak, which gradually disappears with increasing temperature. The position of the small hump in $g_{\text{SbSb}}(r)$ is at 0.43 nm, which is the position of the second-neighbour distance in the crystalline Sb state (rhombohedral A7-structure which originates from a Peierls distortion of a simple cubic lattice [8]).

Given the partial pair correlation functions, it is possible to estimate the partial coordination numbers as

$$N_{\alpha\beta} = \int_0^{R_{\text{Min}}} 4\pi r^2 \rho_{\beta} g_{\alpha\beta}(r) dr \quad (1)$$

where R_{Min} is the coordinate of the first minimum in the partial pair correlation function. The nearest neighbour distance and the calculated partial coordination numbers of l-InSb are summarized in table 1. From table 1, we can find that as temperature is increased, the homogeneous and heterogeneous bonds decrease gradually and the partial coordination numbers become small. To estimate the compositional defects, a compositional disorder number (CDN) [17], defined as the ratio of homogeneous and heterogeneous bonds

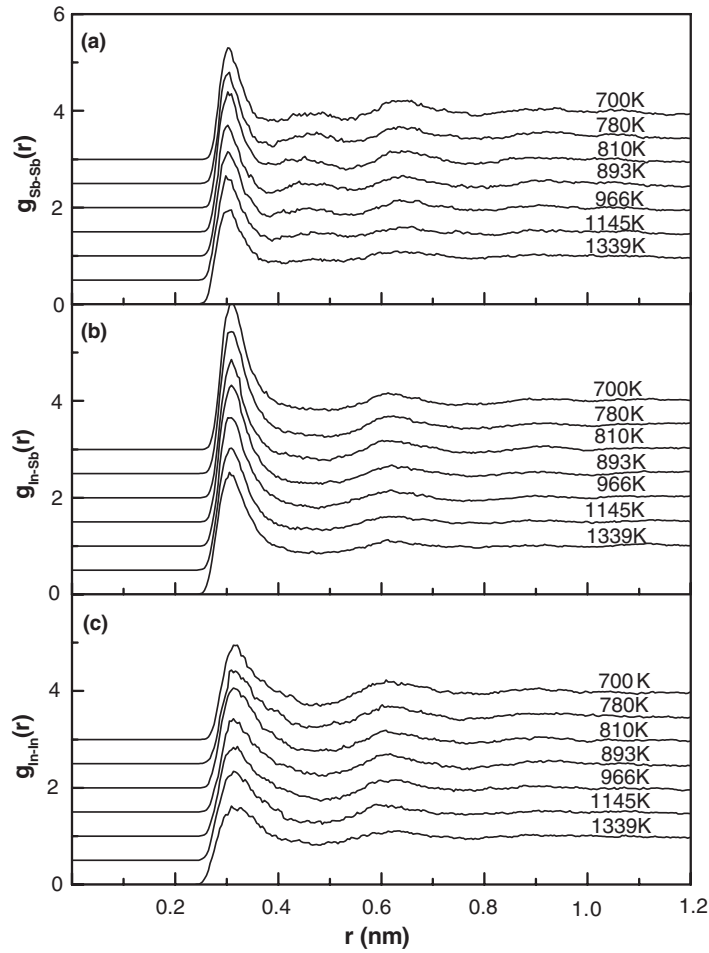


Figure 2. The partial pair correlation functions of liquid InSb alloy.

$(N_{\alpha\alpha} + N_{\beta\beta})/2N_{\alpha\beta}$, is calculated and also illustrated in table 1. The CDN can also be thought of as an order parameter. In c-InSb, CDN is equal to 0. If CDN is equal to 1, it will mean that homogeneous and heterogeneous bonds have the same probability. The greater the number of homogeneous bonds (or the fewer the heterogeneous bonds), the greater the CDN is. As shown in table 1, the CDN is less than 1 in l-InSb, which suggests that heterogeneous bonds still play a predominant role in liquid InSb alloy.

To get a more detailed description of the local atomic configuration, the bond-angle distribution function $g_3(\theta)$, as one type of three-body correlation function, was calculated from the atomic configuration obtained by our simulations. The angle noted in $g_3(\theta)$ is formed by a pair of vectors drawn from a reference atom to any other two atoms within a sphere of cutoff radius r_{cutoff} . As the directionally covalent bonds of Sb–Sb partially exist in l-InSb, it may provide more detailed information about the microscopic structure of l-InSb. Figure 3 presents the calculated bond-angle distributions $g_3(\theta)$ of the Sb atoms. Here, to emphasize the deviation from a random distribution, the bond-angle distributions are normalized by $\sin \theta$. Our $g_3(\theta)$ with the cutoff distance of 0.34 nm (i.e. including essentially the symmetric part of the first peak of $g_{\text{SbSb}}(r)$) is rather broad with two peaks at $\theta \sim 90^\circ$ and $\theta \sim 180^\circ$, indicating the

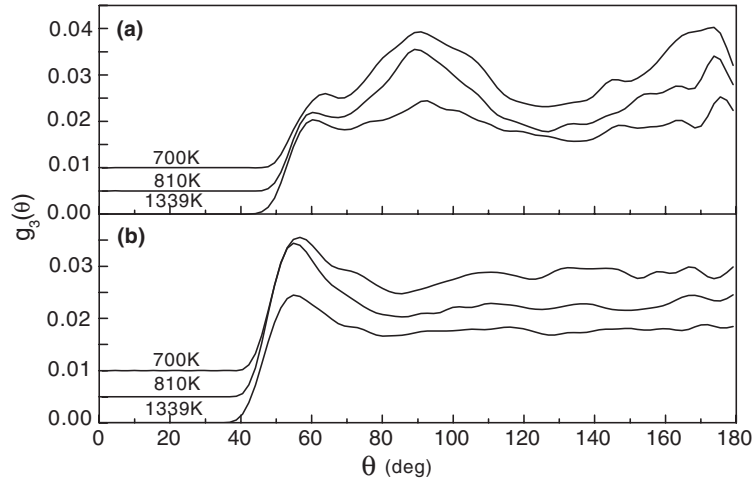


Figure 3. Bond-angle distributions of Sb clusters in liquid InSb alloy: (a) SbSbSb with $r_{\text{cutoff}} = 0.34$ nm; (b) SbSbSb with $r_{\text{cutoff}} = 0.43$ nm.

Table 1. Nearest-neighbour distance, partial coordination number and compositional disorder number (CDN) of liquid InSb alloy.

T (K)	r_{InIn} (nm)	N_{InIn}	r_{InSb} (nm)	N_{InSb}	r_{SbSb} (nm)	N_{SbSb}	CDN
700	0.313	4.1	0.309	5.2	0.302	2.3	0.62
780	0.313	4.1	0.309	5.1	0.302	2.2	0.62
810	0.313	4.1	0.309	5.0	0.302	2.2	0.63
893	0.313	4.1	0.309	4.9	0.302	2.2	0.64
966	0.313	4.0	0.309	4.8	0.302	2.1	0.64
1145	0.313	4.0	0.309	4.6	0.302	2.1	0.66
1339	0.313	3.7	0.309	4.6	0.302	2.0	0.62

existence of rectangular and opened chain-like structures in Sb–Sb bonds. This result is in good agreement with that of Seifert *et al* for liquid Sb [8]. Seifert *et al* regarded the nearest neighbour configuration of l-Sb as a weak Peierls distortion with only a gradual difference between the short and the long bonds. With a cutoff distance of 0.43 nm, equal to the distance of the next-nearest neighbour of crystalline state Sb, only one peak at $\theta \sim 60^\circ$ appears in the $g_3(\theta)$, corresponding to the angle between next-nearest-neighbour bonds in a weakly Peierls distorted simple cubic structure. The height of these three peaks decreases with increasing temperature. Thus, the local structures of Sb atoms in l-InSb are partly similar to those in liquid Sb, and with increasing temperature the extent of this similarity is gradually weakened.

Figure 4 shows snapshot pictures of the distribution of Sb atoms in l-InSb at three different temperatures. To simplify the visualization of the pictures, only atoms of Sb and bonds between them are shown. Two atoms are said to be near neighbours, or are considered to be bonded (be connected by a stick in figure 4), if the pair of atoms is closer than a specific cutoff distance, chosen to be 0.34 nm, i.e. the first minimum of $g_{\text{SbSb}}(r)$. From figures 4(a)–(c), one can see clearly that with increasing temperature the opened chain-like Sb–Sb bonds are broken, the number of bonded Sb–Sb pairs decrease and the cluster size formed by bonded Sb atoms decreases, which is in agreement with the above result for N_{SbSb} .

In order to further investigate the local structure of Sb atoms in liquid InSb alloy we plot in figure 5 the angular limited triplet correlation function as introduced in [1]. This function,

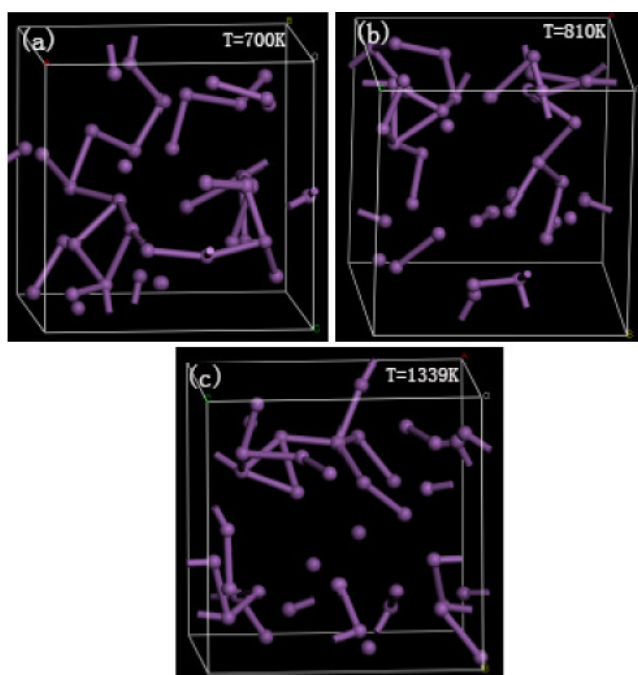


Figure 4. Snapshots of the structure of liquid InSb alloy. Only atoms of Sb and bonds between them are shown in supercell geometry: (a) $T = 700$ K; (b) $T = 810$ K; (c) $T = 1339$ K.

(This figure is in colour only in the electronic version)

$P(r_1, r_2)$, is defined as the probability of finding an Sb atom at r_2 from an Sb atom which is at a distance r_1 from a reference Sb atom. For an undistorted disordered structure, the maximum of the distribution should be on the diagonal (i.e. a maximum at $r_1 = r_2$). For liquid InSb alloy at 810 K, shown in figure 5(a), the maxima of the distribution are located at (0.312 nm, 0.322 nm) and (0.322 nm, 0.312 nm), which shows correlation of longer and shorter bonds (the signature of the Peierls distortion mechanism). Some smaller regions, centred at (0.325 nm, 0.288 nm), (0.320 nm, 0.290 nm) and (0.313 nm, 0.295 nm), and their symmetric regions also show a tendency to alternate long and short bonds. Another region of strong correlation is centred at (0.304 nm, 0.304 nm), which approximately corresponds to the position of the first peak in the partial pair correlation function $g_{\text{SbSb}}(r)$. Figure 5(a) shows the correlation of longer and shorter bonds in l-InSb at 810 K, which is in good agreement with the calculation result of Gu *et al* [1]. For liquid InSb alloy at 1339 K, shown in figure 5(b), only one maximum of the distribution is shown at (0.304 nm, 0.304 nm), i.e. the same bonds, which suggests an undistorted disordered structure. From figure 5 we can see clearly that the structure of liquid InSb alloy near the melting points is very complex, and the Peierls distortion is weakened as temperature increases.

3.2. Dynamic properties

We have studied the dynamic properties of liquid InSb alloy from a supercooled temperature of 700 K to 1339 K by calculating the mean square displacement (MSD), defined in the

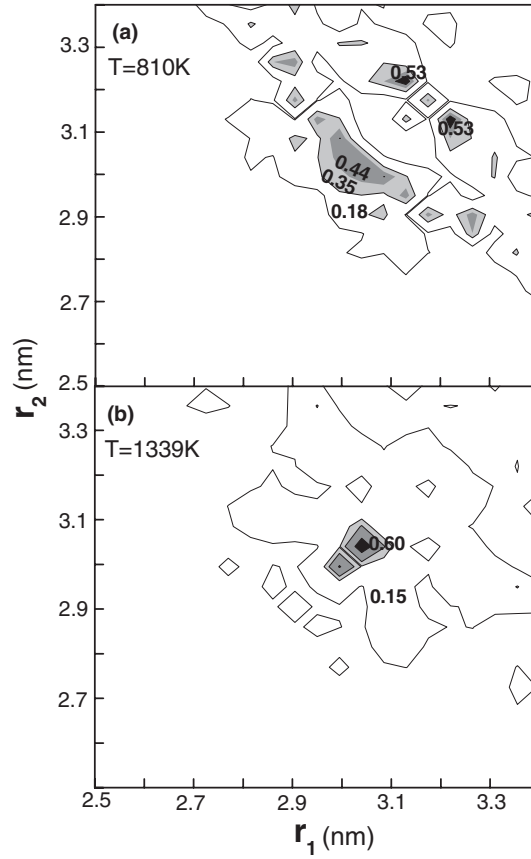


Figure 5. Angular limited triplet correlation functions $P(r_1, r_2)$ of Sb–Sb–Sb in liquid InSb alloy.

conventional way:

$$\langle \Delta \vec{r}(r)^2 \rangle = \frac{1}{N_\alpha} \langle |\vec{r}_{i\alpha}(t + t_0) - \vec{r}_{i\alpha}(t_0)|^2 \rangle \quad (2)$$

where summation goes over all N_α of the α species, \vec{r}_i is the coordinates of atom i and t_0 is the arbitrary origin of time; the average is taken for all possible t_0 . In the liquid state, the behaviour of the MSD in the long time limit is proportional to time, which is correlated with the diffusion coefficient D_α by the so-called Einstein relationship:

$$D_\alpha = \frac{1}{6t} \langle \Delta \vec{r}_\alpha(t)^2 \rangle \quad (3)$$

where D_α is the diffusion coefficient of the α species. According to the Einstein relationship, we can easily calculate the diffusion coefficients of In and Sb in liquid InSb alloy. We further calculate the diffusion coefficients of liquid InSb alloy by the following relation:

$$D = \frac{D_{\text{In}} + D_{\text{Sb}}}{2}. \quad (4)$$

In figure 6, the natural logarithm of D is plotted as a function of the reciprocal of temperature ($1/T$). We can clearly see that the dependence of the diffusion coefficient on temperature follows the Arrhenius relationship:

$$D = D_0 e^{-\frac{E_\alpha}{k_B T}} \quad (5)$$

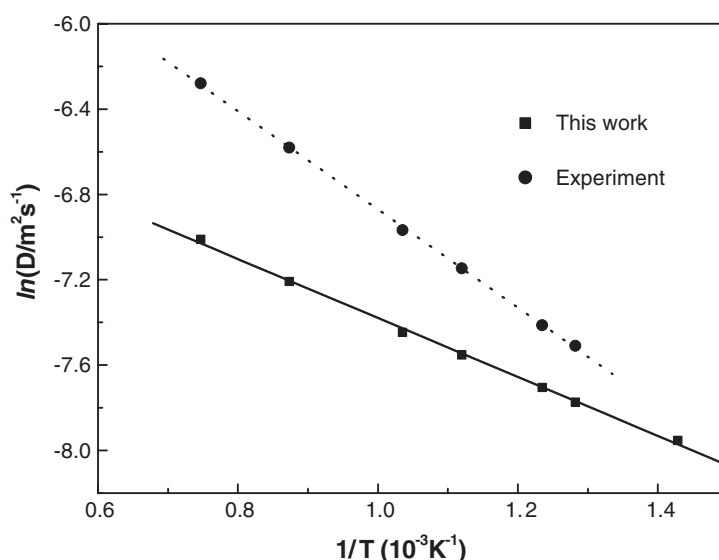


Figure 6. The temperature dependence of the diffusion coefficient for liquid InSb alloy. The ‘experimental’ data for the diffusion coefficient are calculated using the viscosity coefficient from [10]. The solid and dotted lines are curve fits obtained assuming Arrhenius behaviour.

where E_a is the activation energy, T is the temperature, D_0 is the pre-exponential factor and k_B is the Boltzmann constant. By a linear fit of $\ln D$ via $1/T$ (figure 6), the obtained E_a and D_0 are 0.20 eV and $2.01 \times 10^{-8} \text{ m}^2 \text{ s}^{-1}$, respectively, for liquid InSb alloy. Unfortunately, there is no direct experimental data for the diffusion coefficient. In order to make a comparison of our calculations and the experimental results, the ‘experimental’ values of the diffusion coefficient are calculated from the experimental data of the viscosity coefficient of l-InSb [10] using the Stokes–Einstein relationship:

$$\eta = \frac{k_B T}{2\pi a D} \quad (6)$$

where a is the effective ‘diameter’ of the diffusing particles. We select the particle size as the position coordinate of the first peak of the pair correlation function, defined as the average value of the nearest-neighbour distance. The ‘experimental’ values of the diffusion coefficient at different temperatures are also presented in figure 6. One can see that the temperature dependence of the diffusion coefficient of l-InSb is in good agreement with that of the ‘experimental’ data in overall tendency, and shows a linear relationship, though our calculated diffusion coefficients of l-InSb are always less than that the ‘experimental’ values. A similarly linear fit of the ‘experimental’ data is quite satisfactory and yields a value for activation energy of 0.31 eV and a value of the pre-exponential of $8.41 \times 10^{-8} \text{ m}^2 \text{ s}^{-1}$, which may be compared with our theoretically obtained values.

To check the dependence of the diffusion coefficient on the size of the system, we have performed AIMD simulations of l-InSb at 810 and 1339 K using a larger system composed of 120 atoms. The diffusion coefficients of the 120-atom system are about 4.5% and 6.8% larger, respectively, than that calculated for the system of 80 atoms. This shows that the finite-size effects are expected to be small.

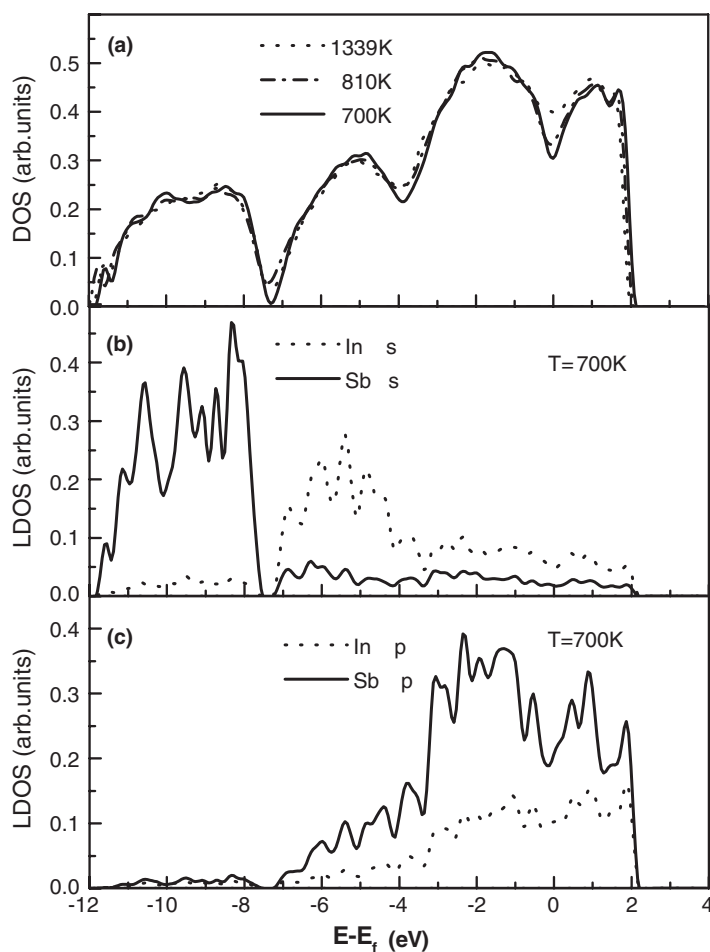


Figure 7. The total electronic density of states and the local density of states ($T = 700$ K) for liquid InSb alloy.

3.3. Electronic properties

To study the variation of electronic structure with temperature, the electronic density of states (DOS) and the local density of states (LDOS) are calculated. The LDOSs are obtained by projecting the wavefunctions onto spherical harmonics centred on each atom with a radius of 0.144 nm for In atoms and 0.140 nm for Sb atoms (covalent radius tabulated in most periodic tables). The total DOSs from 700 to 1339 K and the LDOSs at a supercooled temperature of 700 K are displayed in figure 7. The total DOS is very similar in figure 7(a). The gap at the Fermi level disappears, although a small ‘dip’ is preserved, indicating that supercooled liquid and normal liquid InSb alloys demonstrate metal-like behaviour. As the temperature increases, the ‘dip’ in the total DOS decreases quickly. From figures 7(b) and (c) we can see that peaks near -5 and -8.5 eV in the DOSs are mainly formed by the In(s) and Sb(s) bonding orbitals, respectively, but the peaks near -1.5 , 1.0 and 2.0 eV result from the overlap of the In(p) and Sb(p) orbitals, respectively. The DOSs and LDOSs of l-InSb are not altered drastically from a supercooled temperature of 700 K to 1339 K.

4. Conclusions

We have performed AIMD simulations of liquid InSb alloy from a supercooled temperature of 700 K to 1339 K. Analysis of the local structure of Sb atoms in l-InSb alloy clearly shows that with increased temperature the opened chain-like Sb–Sb bonds are broken, the localized atoms become free, the cluster size of Sb atoms decreases and the Peierls distortion of Sb atoms in l-InSb is weakened. Although homogeneous bonds appear in l-InSb, the heterogeneous bonds are still superior to them. The structure of l-InSb near the melting point is complex, and may cause anomalous changes in physical properties. The DOS and LDOS calculations show normal liquid and supercooled liquid InSb alloys to exhibit metallic-like behaviour. The temperature dependence of the diffusion coefficient of l-InSb shows an Arrhenius-type behaviour, which is in good agreement with the experimental results of Sato *et al* [10].

Acknowledgments

This work was supported by the National Natural Science Foundation of China (no. 10374089) and the Knowledge Innovation Program of Chinese Academy of Sciences (no. KJCX2-SW-W17). We would like to thank the Center for Computational Science, Hefei Institutes of Physical Sciences.

References

- [1] Gu T, Bian X, Qin J and Xu C 2005 *Phys. Rev. B* **71** 104206
- [2] Zhang C, Wei Y and Zhu C 2005 *Chem. Phys. Lett.* **408** 348
- [3] Hattori T, Kinoshita T, Taga N, Takasugi Y, Mori T and Tsuji K 2005 *Phys. Rev. B* **72** 064205
- [4] Gaffney K J *et al* 2005 *Phys. Rev. Lett.* **95** 125701
- [5] Phillips G 1973 *Bonds and Bands in Semiconductors* (New York: Academic)
- [6] Rino J P, Borges D S and Costa S C 2004 *J. Non-Cryst. Solids* **348** 17
- [7] Wang Y, Lu K and Li C 1997 *Phys. Rev. Lett.* **79** 3664
- [8] Seifert K, Hafner J and Kresse G 1996 *J. Non-Cryst. Solids* **205–207** 871
- [9] Glazov V M, Chizhevshaya S N and Glagoleva N N 1969 *Liquid Semiconductors* (New York: Plenum)
- [10] Sato Y, Nishizuka T, Takamizawa T, Yamamura T and Waseda Y 2002 *Int. J. Thermophys.* **23** 235
- [11] Kresse G and Furthmüller J 1996 *Comput. Mater. Sci.* **6** 15
- [12] Kresse G and Furthmüller J 1996 *Phys. Rev. B* **54** 11169
- [13] Wang Y and Perdew J P 1991 *Phys. Rev. B* **44** 13298
- [14] Kresse G and Hafner J 1994 *Phys. Rev. B* **49** 14251
- [15] Nosé S 1984 *J. Chem. Phys.* **81** 511
- [16] Verlet L 1967 *Phys. Rev. B* **159** 98
- [17] Godlevsky V and Cholikowsky J R 1998 *J. Chem. Phys.* **109** 7312